International Journal of Research Studies in Electrical and Electronics Engineering (IJRSEEE)
Volume 6, Issue 3, 2020, PP 1-15
ISSN 2454-9436 (Online)
DOI: http://dx.doi.org/10.20431/2454-9436.0603002
www.arcjournals.org

Impedance of Skin-Plasma Effect

Ordin S.V

Ioffe Institute RAS

***Corresponding Author: Ordin S.V,** *Ioffe Institute RAS*

Abstract: *The scale of nanoelements has raised the question of the applicability of some well-known optical models. And the analysis of the limits of their applicability showed that the work begun by Planck on the elimination of false singularities in the functions used in physical models has not been completed in many respects. In this regard, the reaction of free electrons to radiation was also previously described in a fragmentary-classical way, within the framework of the skin effect and plasma reflection, which led to a kind of ultraviolet and infrared catastrophe.*

Understanding the general problem required the elimination of this fundamental "catastrophe", and not with the help of corrections of the "anomaly" type used, in principle, of the same models. Normalization of the frequencies of emission and decay of electrons to the plasma frequency made it possible to obtain a general qualitative picture of the dynamic electron response to radiation in the form of a semiempirical size-dependent function of generalized skin-plasma absorption, a kind of Planck function for real decaying plasmons.

An in-depth analysis of this function led to an understanding of the fundamental feature of describing the dynamics of free electrons using the well-known electrical impedance, traditionally perceived as a purely radio-technical parameter, but in reality giving a more complete description of a harmonic oscillator than a purely mechanical oscillator.

So the generalization of the models describing the reaction of free carriers to radiation one-sidedly led to the need to take into account not only Quantum Mechanics, but also Quantum Electronics. The analysis of the Foundations of the newly created Quantum Electronics revealed that the final impedance of the vacuum determines the minimum attenuation and thus the boundary of the physical values of the models used. In general terms, it is the vacuum impedance that determines both the complexity of the refractive index of the vacuum and the maximum visibility limit in the Universe.

On the basis of the described boundary effect on free electrons, optimizing the geometric nano-dimensions in weakly absorbing media within the framework of the obtained model, it is possible to create fundamentally new active bipolar elements of electronics.

Keywords: *plasma reflection, skin effect, model applicability limits, Planck function, oscillatory circuit, New Quantum Electronics.*

1. PLASMA REFLECTION ANALYSIS

Planck, in his generalizing theory of the radiation of the Absolute Black Body, considered the idealized case of persistent resonant photons and, revealing a fundamentally new ELEMENT - Quantum. Thus, passing from a continuous set to a countable one, he eliminated false singularities and gave a unified description of thermal radiation. But he eliminated them only in this idealized case, and the descriptions of some specific effects in their theories, including those directly conjugated with Planck's model, remained uncombed. And not only in theories that are a compilation of the quantum and classical approaches. But even some purely classical and actively used models remained at the pre-Planck level. So false singularities can be seen on the example of two models / approaches describing the optical properties of free electrons in a solid.

Namely, when the frequency of the excited radiation tends to zero, the plasma model of free electrons gives in the region adjacent to the zero frequency a negative real part of the dielectric constant ε_1 (Fig. 1a), which determines the reflection coefficient R close to 100% (Fig. 1b).

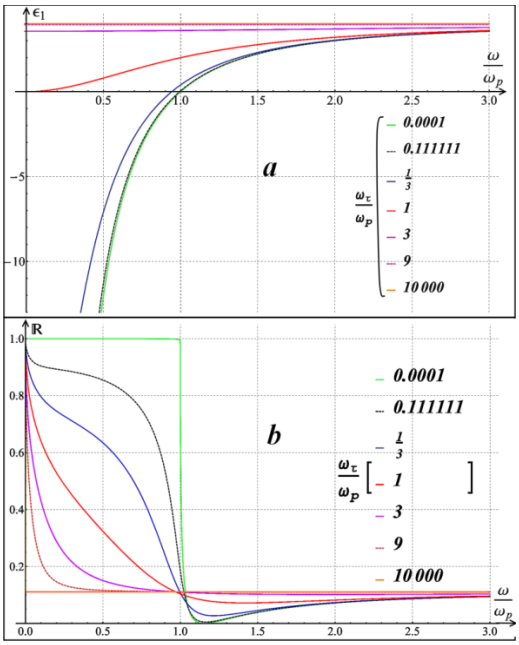

Fig1. *Dependence of the real part of the dielectric constant* ε_1 *(a) and the reflection coefficient* ***R*** *on the reduced frequency* ω/ω_p *at different values of the relative attenuation* ω_τ/ω_p *of the free carrier plasma*

And this, built on the basis of the classical Drude-Lorentz model, the plasma reflection model is widely used to describe the reflection from various conductive materials [1. And as follows from the Drude-Lorentz model, the plasma frequency ω_P, the frequency of the zero crossing of the real part of the permittivity (Fig. 1a), corresponding to the oscillation along the boundary of the conducting medium, called the longitudinal resonance. It corresponds to the reaction of the entire set of electrons with an average collision time, which determines its relationship with both the conductivity $\sigma(0)$ at direct current and the concentration of electrons n and the mass of an electron m_e at low frequencies

$$\omega_P^2 = \frac{4\pi\sigma(0)}{\varepsilon_\infty \tau} = \frac{e^2 \cdot n}{\varepsilon_\infty \cdot m_e} \tag{1}$$

As the damping increases, as shown in Fig. 1a, the real plasma frequency decreases

$$\left(\omega_P^*\right)^2 = \omega_P^2 - \frac{1}{\tau^2} = \omega_P^2 - \omega_\tau^2, \tag{2}$$

vanishing when the frequency of the longitudinal resonance of the sustained plasma is equal to the frequency of collisions of electrons. But plasma resonance is a resonance for a charge density wave and when irradiated with neutral light corresponds to a wave along the surface of a conducting medium. The total wave vector of this “circular” surface wave is zero, which ensures its interaction with light and a charge addition to the zero resonance frequency of free electrons. In this case, the plasma resonance manifests itself directly as a mechanical one only if there are boundaries in the path of this wave, as, for example, will be shown in Fig. 3, or upon excitation by charged particles.

In the absence of boundaries perpendicular to the electric field of the wave incident on the surface, the resonant frequency of free-carrier oscillations with low damping is strictly zero, as for any mechanical oscillator with zero restoring force:

$$\frac{d^2x}{dt^2} + \gamma \frac{dx}{dt} = \frac{F}{m} \tag{3}$$

Whereas for damped oscillations, friction somewhat lowers the real plasma frequency due to the shift of the mechanical resonance frequency ω_0 to the imaginary region.

$$\omega_{\text{Res}} = \left[\sqrt{\omega_0^2 - \frac{\gamma^2}{2m}}\right]_{/\omega_0 \to 0} \Rightarrow i\frac{\gamma}{\sqrt{2m}} \tag{4}$$

But the practically described plasma model should give an absorption peak for a free plasma, as will be shown in Fig. 7, precisely at zero frequency, which contradicts observations.

But before proceeding to the analysis of specific details of the plasma model, let us immediately emphasize its fundamental point. The real part of the dielectric constant (Fig. 1a), which determines the large reflection for free carriers (Fig. 1b), is assumed in the optical model to change abruptly in an infinitely thin surface layer in comparison with the wavelength. In this case, the internal structure of this layer, naturally, is not considered, i.e. and does not take into account the periodicity of waves and atomic structure in it [2].

So, in the consideration shown in Fig. 1, the scale of this "optical" layer was not taken into account at all. Whereas the imaginary part of ε_2 and, accordingly, the absorption coefficient α are introduced as the specific (per unit length of the path traveled by the light) characteristic of the volume of the conducting material! But it is this volumetric frequency dependence that is associated, according to the principle of causality, with the frequency dependence of the surface jump of the real part of the permittivity! Those. The full frequency dependence of the real part of the dielectric constant shown in Fig. 1a is associated by the Kramers-Kronig relation only with the determined frequency dependence of its imaginary part.

However, the optical reflection spectra of perfect crystals and homogeneous alloys processed according to this plasma model coincide so well with the experimental spectra in the IR region that they have long been used as basic ones for contactless determination of the concentration and mobility of free carriers [3]. In this case, their divergences / deviations even allow one to reveal additional energy-selective features in the scattering of free carriers (impurity levels and interband transitions) against the background of pure plasma reflection (Fig. 2).

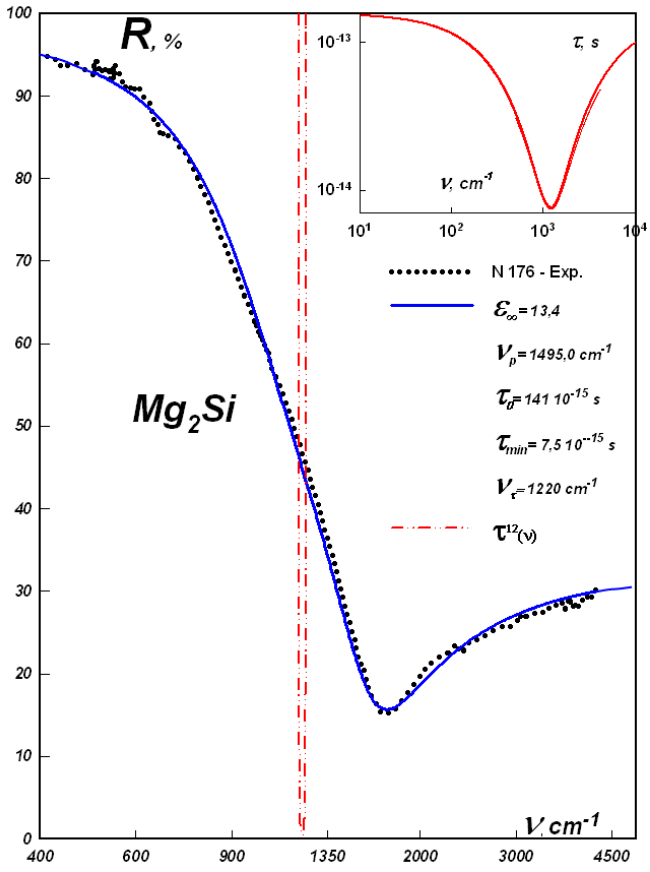

Fig2. *Plasma reflection spectrum of heavily doped Mg_2Si semiconductor*

Those.in the near- and mid-IR, the thickness of the optical boundary in semiconductors is indeed negligible and can be neglected.

Interference effects have been studied and used for a long time [4], while diffraction effects were previously considered only as surface effects [5]. But, as shown by studies of a diffraction grating formed on a fluorite crystal with a thickness and a step of 500 nm, and the volume reflection coefficient depends on the wavelength - it has a maximum when the light is polarized perpendicular to the metal strokes and the frequency edge of reflection during polarization along the grooves, determined by the scale of the region by the spatial localization of free electrons and the period of the diffraction grating (Fig. 3).

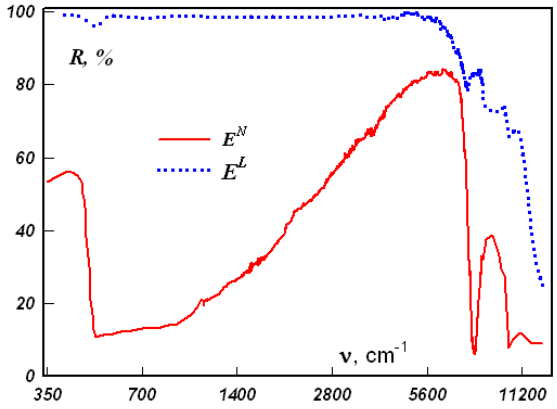

Fig3. *Spectra of normal reflection modelling nanostructures at orientation of electric vector* ***E*** *in parallel* ***(E^L)*** *and it is perpendicular* ***(E^N)*** *to metal strings.*

The need to take into account in principle the influence on the real part of the dynamic conductivity of interference effects on the concentration layer modulation in one-dimensionally incommensurate crystals, an influence that cannot be described using Landau's smallness corrections, was first shown in [6].

Thus, the high-frequency lattice oscillator observed at $\boldsymbol{E^N}$ (Fig. 3) possibly corresponds to the oscillations of a plasma localized across the high-conducting layer. At $\boldsymbol{E^L}$, a longitudinal plasmon appears at the same effective frequency.

But qualitatively, the plasma model for free carriers with crystal modulations at the atomic level is in good agreement with high reflectivity in the IR range of both semiconductors (Fig. 2) and graphite (Fig. 4), and highly conductive metals such as silver, copper, and aluminum. (fig. 6). At the same time, for graphite (Fig. 4), the model plasma fit gives good qualitative and quantitative agreement with experiment in a very wide spectral range, which, as shown below, makes it possible, in principle, to clarify the mechanisms of the conduction of graphite.

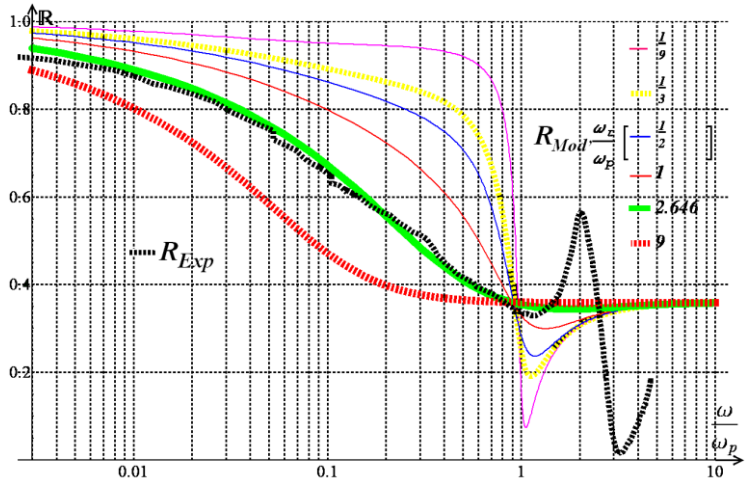

Fig4. *Fitting the model reflection on plasma oscillations to the experimental reflection spectrum of a highly conducting face - the crystal cleavage plane (perpendicular to the C axis) of rhombohedral graphite*

Taking into account the higher-frequency than plasma contributions to the reflection coefficient by free carriers only to the real part of the dielectric constant ε_∞, this model gives the frequency dependence of the reflection coefficient:

$$R(x)=\frac{1+\varepsilon_\infty\sqrt{1+\frac{1-2x^2}{x^2\left(x^2+\xi^2\right)}}-\sqrt{2\varepsilon_\infty}\sqrt{1-\frac{1}{x^2+\xi^2}+\sqrt{1+\frac{1-2x^2}{x^2\left(x^2+\xi^2\right)}}}}{1+\varepsilon_\infty\sqrt{1+\frac{1-2x^2}{x^2\left(x^2+\xi^2\right)}}+\sqrt{2\varepsilon_\infty}\sqrt{1-\frac{1}{x^2+\xi^2}+\sqrt{1+\frac{1-2x^2}{x^2\left(x^2+\xi^2\right)}}}}, \quad (5)$$

Where $x=\frac{\omega}{\omega_P}$ is the reduced frequency, and $\xi=\frac{\omega_\tau}{\omega_P}$ is the reduced damping frequency. And this model reflection coefficient describes well in a wide frequency range the reflection from the surface of both weakly conducting semiconductors (Fig. 2) and highly conducting atomic layers of a rhombohedral graphite crystal (Fig. 4).

Figure 5 shows the optimal fit of the graphite reflection, which was obtained at $\varepsilon_\infty\cong16$ and at $\xi\cong2.646$ a fairly high plasma wavenumber $\nu_P=\frac{1}{\lambda_P}=\frac{\omega_P}{2\pi c}\approx20000\,cm^{-1}$, which is numerically related to the ratio of the concentration of free carriers n to their effective mass m^*:

$$\frac{n\left[cm^{-3}\right]}{m^*}\approx\varepsilon_\infty\left(\frac{\nu_P\cdot10^6}{0.3}\right)^2=4\left(\frac{20000\cdot10^6}{0.3}\right)^2=\frac{16}{9}10^{22}=1.77778\cdot10^{22} \quad (6)$$

Assuming that in semimetal graphite the number of holes is equal to the number of electrons and taking the arithmetic mean of their effective masses given in the literature - 0.05, we obtain the concentration of electrons / holes

$$n_{e/p}\approx\frac{0.05}{2}1.77778\cdot10^{22}=4.44444\cdot10^{20}\,cm^{-3} \quad (7)$$

The resulting concentration of charge carriers in plasma is about three orders of magnitude less than that of metals, but about two orders of magnitude higher than that attributed to graphite in the literature, and even if we put their effective mass equal to unity, it is still an order of magnitude higher. In this case, the free path of these carriers is short:

$$\tau\approx\frac{1}{c\cdot2.646\cdot\nu_P}=6.29882\cdot10^{-16}\left[c\right] \quad (8)$$

And so, the optical plasma model works quite precisely in semiconductors, where it is one of the most proven instruments for determining the concentration and free path of current carriers. For a semimetal graphite, it also quite accurately describes the reflection coefficient from ultraviolet to far infrared. In this case, this model used also shows that, in addition to the highly mobile electrons and holes with a concentration of 10^{18} cm^{-3}, which are usually taken into account in graphite, low-mobile carriers with a concentration higher by about two orders of magnitude also participate in the formation of its plasma reflection. But this high concentration of electrons is three orders of magnitude less than if the conductivity along the monoatomic planes of graphite would provide the electron π-bond of each atom.

Moreover, the high-frequency reflection peak shown in Fig. 5 in graphite in metals is usually attributed to interband transitions. But the high-frequency "king" at the edge of the plasma reflection of graphite provides additional information about electrons. Since it is located strictly at the doubled

plasma frequency, it corresponds to the highest plasma concentration by an electron, but at the same time localized - an electron with a hole form a dipole (not to be confused with the accompanying electron polarization of the crystal lattice, called a polaron).

Thus, a high-frequency size dependent effect is directly observed on graphite in the optical permittivity itself - the transition from its determination through the internal field

$$\varepsilon_{internal} = \frac{E_{internal}(\omega) + 4\pi\rho(\omega)}{E_{internal}(\omega)} \tag{9}$$

which gives for free carriers a transverse resonance mode at zero frequency, to its definition through an external field and a polarization field

$$\varepsilon_{external} = \frac{E_{external}(\omega)}{E_{internal}(\omega) - E_{polarization}(\omega)} \tag{10}$$

which gives a longitudinal resonance mode just at the plasma frequency. But this is a high-frequency, size-dependent effect corresponding to local oscillations of individual electrons relative to the nearest ion. At the low-frequency edge, there is a transverse (to the radiation wave vector) oscillation of the set of all electrons - the current relative to the entire ionic core of the crystal lattice, corresponding for infinite dimensions to the zero resonance frequency, and for finite dimensions - to low-frequency resonances, which have long been used in antenna resonance.

It follows from the above analysis that direct current conductivity along monoatomic graphite layers is provided by two sliding (with friction) sublattices of electrons and holes with a concentration of approximately one electron-hole pair per thousand atoms. But at high frequencies this electron-hole "crystal" structure has its own optical phonons.

These electron-hole oscillations provide $\varepsilon_\infty \cong 4$ for low-frequency plasma. So, in the graphite layers, it is energetically more favorable to form an electron-hole two-dimensional crystal lattice, rather than through orbits of free electrons, which imply mystical infinite conductivity.

And so, the optical plasma model, which quantitatively describes well the behavior of free carriers in semiconductors, qualitatively and for graphite, in principle, well describes the reflection in a very wide frequency range, but requires correction of the mechanism of current generation. In principle, it was originally intended for highly conductive isotropic metals for the qualitative separation of a wide range of plasma reflection frequencies from the higher frequency range of their UV transparency, where their spectral features were mainly associated only with local effects on electrons bound to atoms, on electron atomic orbitals. (Fig.5).

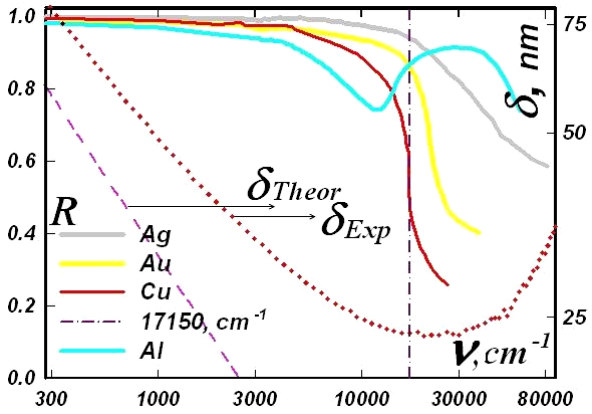

Fig5. *Spectral dependences (1 cm $^{-1}$ ≈ 3 10 ^{10} Hz) of the reflection coefficients of highly electrically conductive metals (solid lines) and the thickness of the copper skin layer (red dots - experiment, pink dashed line - theory).*

In this case, as can be seen from Fig. 6, a significant deviation of the reflection coefficient of metals from the monotonicity of the model one is present only in aluminum. It is this dip in the reflection coefficient that leads to errors in many spectral measurements at the border of visible and infrared

radiation, since the devices mainly use aluminum mirrors, on which multiple reflections occur, which significantly attenuates the signal. Therefore, I use freshly polished silver mirrors as a reference mirror in my high-precision, wide-range IR measurements involving the visible range. The plasma edge is most clearly manifested in the reflection coefficient of copper, which makes it possible to estimate with good accuracy the plasma frequency of copper from the maximum (in absolute value) of the derivative of its reflection coefficient. However, in the experimental spectral dependence of the copper skin layer thickness $\boldsymbol{\delta}$ (red dots) shown in Fig. 6, a decrease in its thickness at low frequencies does not correspond to the frequency dependence of the reflection, but, on the contrary, an increase in transparency. At frequencies above the plasma frequency, the onset of the so-called ultraviolet transparency, which correlates with the experimental dependence of the copper skin layer, directly contradicts the theory of the skin layer (pink dashed line in Fig. 5).

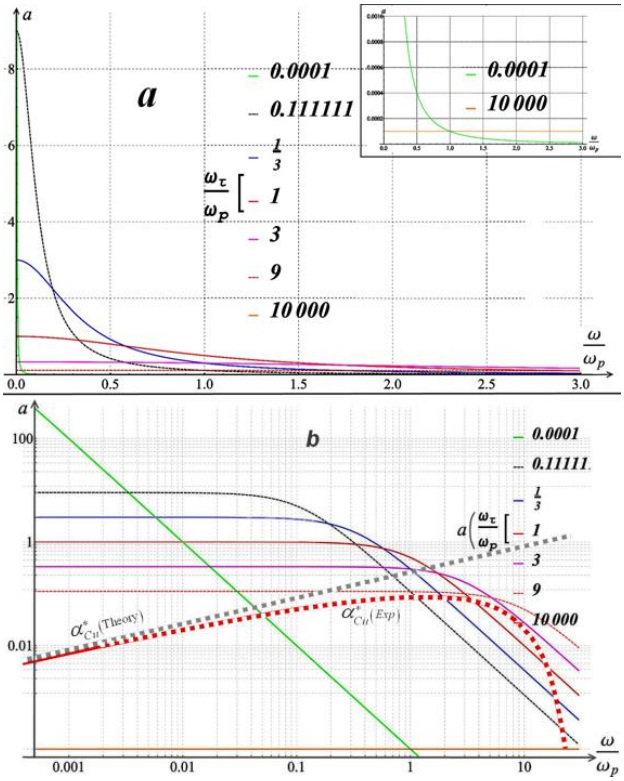

Fig6. *Frequency characteristics of the model plasma absorption on free carriers at their different attenuations and the maximum absorption of copper (red dots).*

And so, the optical model of plasma reflection reliably operates in a wide frequency range and allows one to determine many parameters of a solid. But strictly in accordance with the zero resonance frequency of free carriers, this optical model gives, as shown in Fig. 5, near the zero frequency not only the maximum reflection coefficient (Fig. 1), but also, as shown in Fig. 7, the maximum absorption coefficient $\boldsymbol{\alpha}$, described expression:

$$\alpha = \frac{\varepsilon_\infty \omega_p}{c_0} \cdot \frac{\omega_\tau / \omega_p}{\left(\omega/\omega_p\right)^2 + \left(\omega_\tau/\omega_p\right)^2} = a_0 \cdot a \qquad (11)$$

And this absorption maximum at zero frequency, as shown in Fig. 7a (on a linear scale) and in Fig. 7b (on a double logarithmic scale), is narrow at a low damping frequency ω_τ / ω_p (at long mean free paths, as, say, in semiconductor crystals) and is strongly blurred at a high damping frequency (as in the same metals). The presence of powerful, namely, low-frequency absorption follows, according to the principle of causality, from a large plasma reflection - a large reflection coefficient is associated by the principle of causality and with a large absorption coefficient.

Those. In accordance with Kirchhoff's law in the low-frequency region, the total reflection region according to the plasma model, the transmission tends to zero, which directly contradicts the

experimental spectral dependence of the copper skin layer thickness δ shown in Fig. 5b. And the theory, strictly according to electrodynamics, gives a skin effect with a frequency dependence of absorption, which gives complete transparency, and not a maximum absorption of metals at zero frequency (Fig. 6a). And the electrodynamic approach also agrees well with experiment, say for copper from one Hertz to 10^{13}.

2. SKIN ABSORPTION ANALYSIS

Historically, the region of the lowest frequencies, where the "catastrophe" of plasma reflection actually occurs, was investigated using the so-called eddy, induction currents or Foucault currents. But the description of the initially observed absorption of electromagnetic waves in the radio range was obtained within the framework of the skin effect, which consistently generalized the observed effects with a slow change in the magnetic field [7]. This allowed the skin technique (Fig. 8), as well as the above-described plasma optical reflection technique, to be brought to the level of precision [8] and widely used for testing the specific electrical conductivity of materials [9]. On the other hand, this technique is also used for the analysis of modulated metal structures [10], similar to the one described above (Fig. 4) used for the analysis of plasma reflection of incommensurate structures in [6]. But at the same time, the skin-method at zero frequencies was repelled not from the absorption maximum, but from ZERO! And the actual maximum it gave at high frequencies, where the actual plasma reflection and absorption vanish.

If the optical approach described above was based on the assumption of an infinitely thin surface layer that forms a jump in the real part of the permittivity due to the reaction at all frequencies, including higher frequencies, then the electrodynamic theory of the skin layer repels from the infinite thickness of the surface layer, which forms reflection at low frequencies. ... Thus, proceeding from diametrically opposite ideas about the surface layer, it was, in fact, neglected in macroscopic calculations, and one or another model was used, the one that gave a similarity to the experimental dependences. But in macroscopic measurements of long-wavelength reflection, of course, it is already necessary to take into account the layer that forms, and not only the classical skin absorption coefficient shown in Fig. 7. Moreover, the reactive part, and not only passive (active) losses, must be taken into account on the nano-scale of modern electronic elements. But in order to move forward correctly, we will analyze the standard skin model in more detail.

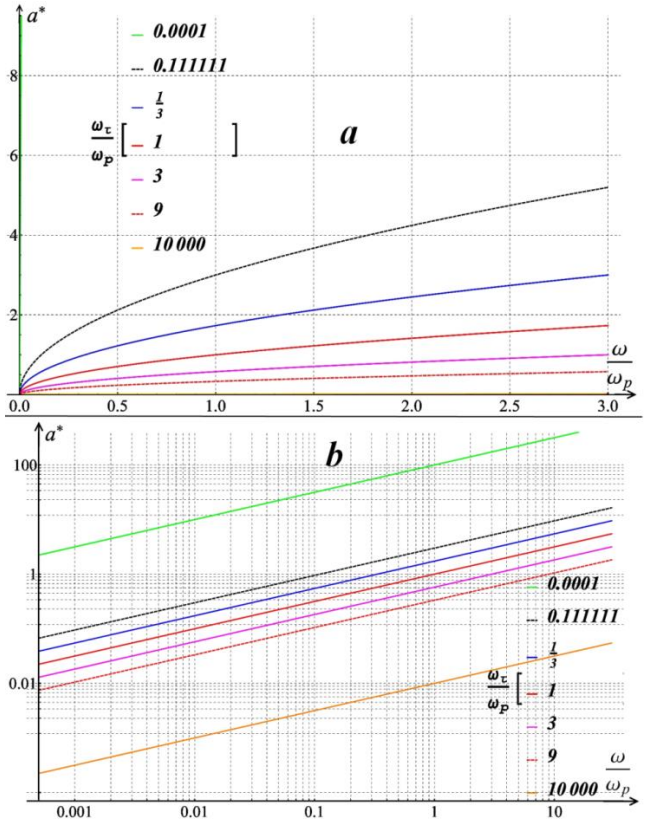

Fig7. *Frequency dependence of the "absorption" of the skin layer (skin absorption)*

The classical absorption of the skin layer shown in Fig. 8 was obtained as the reciprocal of its thickness and expressed in terms of the plasma frequency ω_τ from the Drude-Lorentz model:

$$\frac{1}{\delta_{/\sigma_0}} = \left[\frac{\omega_p}{c_0}\sqrt{\frac{\varepsilon_\infty \mu}{8\pi\varepsilon_0}}\right] \cdot \left[\sqrt{\frac{\omega/\omega_p}{\omega_\tau/\omega_p}}\right] = a_0^* \cdot a^* \qquad (12)$$

In this case, for different approaches / models, we have mutually exclusive frequency dependences of absorption (functions 11 and 12) and their asymptotics (Figs. 7 and 8), which, as already mentioned at the beginning of the section, are diametrically opposite.

So it is obvious that the general electrodynamic approach, when describing the skin effect, was used with some limitations / omissions. Namely, the skin-description of the reaction of free electrons to an electromagnetic wave takes into account only active losses in the medium and does not take into account reactive losses - re-radiation of free carriers, which actually form the reflection R^*, which is widely used in the radio range. So with the received optical transmission recording T

$$T = \left(1 - R^*\right) \cdot \exp(-\alpha^* \cdot d) \ , \qquad (13)$$

The reflection coefficient R^* is neglected, i.e. take it to be zero. The possibility of using this neglect at low frequencies is due to the fact that, as is known, the re-emission of an oscillating charge, proportional to its velocity, rapidly decreases with distance. While the radiation slowly decreasing with distance, which forms the reflection of electromagnetic waves from the metal, is proportional to the acceleration of the charge, i.e. the square of the frequency and, naturally, very little. So the thickness of the layer that forms the reactance of the metal tends to infinity at zero frequencies, and the reflection coefficient R^* actually tends to zero (Fig. 6). Therefore, at the lowest frequencies proportional to the square of the frequency, the low intensity could be neglected. But at the same time, it was assumed that, practically up to the plasma frequency, unaccounted for in the measurements, and in the calculation of the skin absorption by formula 2, the factor (1- R^*), which is close to unity, as shown in Fig. 7, gives only a small error in determining the active losses - actually into absorption.

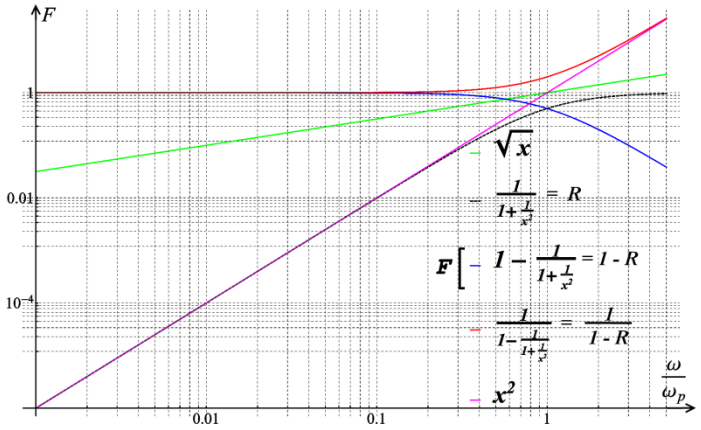

Fig8. *Frequency dependence of skin reflection and its corrections / factors*

But the actual resonance absorption in the vicinity of zero frequency is difficult to measure. And it is technically difficult to measure because of its smallness, determined by its root dependence on the frequency of the skin absorption itself (Form 2 and Fig. 5), and, on the other hand, because of the smearing out of the resonance at small electron mean free paths in metals of the alternative plasma absorption (Fig. 6). This is well known from practice - even copper screens do not provide complete suppression of 50 Hz pickups, and therefore, for precision devices, permalloy screens with a giant magnetic permeability of the order of a million are used. Whereas at sufficiently high frequencies the skin effect itself will be slightly distorted by the frequency dependence of the reflection (Fig. 8), but its contribution to the active absorption itself decreases. Therefore, the root asymptotics of the skin effect (Fig. 7) at high frequencies, in principle, does not work. Whereas with the "abnormality" of the

skin effect, only the size effect was associated, which is actually associated with the frequency dependence of only the active part of the dynamic conductivity, with its dependence on the mean free path of electrons.

Thus, both quantitative (small) corrections to the skin description, and the introduction of a dimensional “anomaly” only for skin absorption, as well as the optical model, do not give a general correct picture of absorption and reflection by free current carriers at any frequencies. Those.fundamental correction and skin models are required.

3. IMPEDANCE ANALYSIS OF ISOTROPIC CONDUCTING MEDIA

Impedance calculations are considered mainly in the theory of waveguides and as a purely technical technique [1, 11, 12, 13]. And for the description of physical processes in both Solid State and Gases I use Mechanical and Quantum-Mechanical Models. Whereas the quantization itself was done by Planck on the example of a waveguide, and the use of impedance to calculate the reflection of waves from a chain of coupled electrical circuits made it possible to qualitatively describe [6] optical "anomalies" in modulated crystals (Fig. 9).

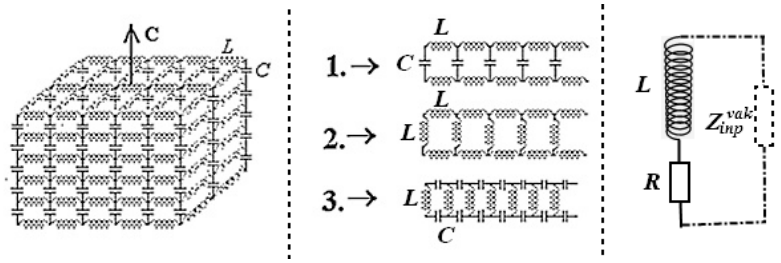

Fig9. *Equivalent waveguide circuit of a crystal with layer conductivity: 1 - the electric vector of light incident on the side face is parallel to the C axis, 2 - the electric vector of light incident on the side face is parallel to the conducting layers, 3 -electric vector of light incident on the face perpendicular to the C axis for any of its polarization is parallel to the conducting layers.*

A thorough analysis of the impedance and its relationship with MEASURABLE parameters: the modulus of the amplitude and phase of the electromagnetic wave, revealed a number of fundamental inaccuracies in its traditional calculations, the elimination of which made it possible to build the Fundamentals of Quantum Nonmechanics.

But the analysis of Quantization is beyond the scope of this article, both in scope and in terms of the problem solved in this article. It will be presented separately, either as a separate article or as a chapter in the book Scientific Advancement of Basic Concepts.

In this article, we will simply consider, with minimal refinements, the traditionally used impedance formulas for the waveguide circuit shown in Fig. 9 under No. 2. In this case, for a conducting isotropic medium, its specific resistance must be included in the equivalent circuit in series, as shown in Fig. 9.

Although the refinements / additions used are of a fundamental nature and were obtained at the output of the noted general analysis, such as, for example, the inclusion in the equivalent circuit of an additional resistance in parallel shown in Fig. 9, which cannot be less than the input impedance of the vacuum, but in relation to the impedance of the conducting medium it is not so essential and we will not consider it.

Impedance, by definition, gives the relationship between the amplitudes and phases of the applied voltage and current.

But by analogy with optics, the complex reflection coefficient of the waveguide is introduced, expressed through the impedance of its reactive elements. So the reflection from the conductive medium is ideally determined by the effective inductance:

$$r_L = \frac{Z_{input}^{vak} - Z_{input}^{L}}{Z_{input}^{vak} + Z_{input}^{L}}, \quad r_{L^*} = \frac{1 - \mathrm{i}\, L^* \omega}{1 + \mathrm{i}\, L^* \omega} \Rightarrow \tag{14}$$

The dependences on the reduced frequency (to the plasma frequency) for all components of the complex reflection coefficient for different values of the inductance reduced to the vacuum impedance, and not only the formally real and imaginary parts, which are often limited in the theory of waveguides, are shown in Fig. 10:

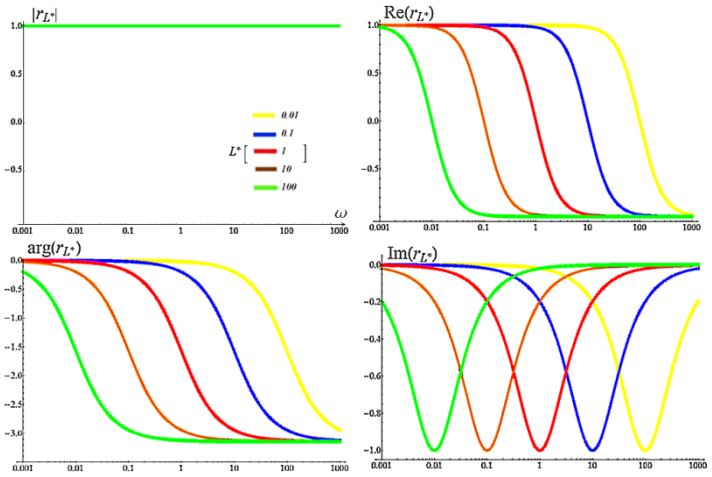

Fig10. *Spectra of the components of the complex reflection coefficient of the reduced inductances of various sizes*

As can be seen from Fig. 10, for any inductance without resistance, the reflection coefficient modulus is characterized by a 100% value at all frequencies with a phase rotation at a reduced frequency equal to the reduced inductance.

The scheme of dividing the medium into cells shown in Fig. 9 itself is arbitrary, but can be tied not only to concentration modulations in the medium [6], but also to other characteristic parameters, say, to the mean free path. This subdivision gives a visual representation of the fact that the electromagnetic wave changes (when subdivided by stepwise jumps) in the transition layer. And for the skin effect - how the phase velocity changes in it and the contributions to the reflected signal are formed, and for the plasma reflection model - how the dielectric constant is formed in the transition layer.

So the response to an incident electromagnetic wave of an infinite chain, which can be obtained by recurrent summation of the contributions to the impedance, for case No. 2 of ideal inductance (say, a superconductor) simply gives an equivalent input inductance of the chain, which is slightly smaller in magnitude than the inductance of the selected element and has the corresponding impedance:

$$Z_{input} = \mathrm{i}\,(\sqrt{3}\text{-}1)\,\mathrm{L}\,\omega \tag{15}$$

If we use the waveguide formula for the reflection coefficient (14), then for this idealized case we obtain a small numerical correction to the inductance. Whereas the introduction of the resistivity of the medium requires taking into account that the re-emission of the wave occurs only due to the inductance energy:

$$r_{L^*} = \frac{1 - iL^*\omega}{1 + iL^*\omega} \cdot Abs\left[\frac{iL^*\omega}{iL^*\omega + R^*}\right] \tag{16}$$

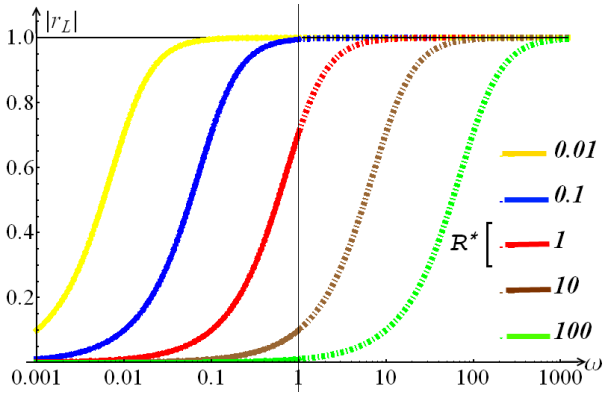

Fig11. *Reflectance spectra of a unit reduced inductance at different resistivities (reduced to vacuum impedance).*

In this case, the modulus of the obtained inductance reflection coefficient, as shown in Fig. 12, tends to unity at high frequencies, at frequencies below the characteristic one, determined by the inductance reduced to vacuum impedance, it drops sharply.

Those.we have a complete reflection of an electromagnetic wave, characteristic of superconductors and in full accordance with the fact that reactive elements do not absorb energy. But, it is interesting that the introduction of a vacuum resistance into this equivalent circuit not only as an input (in f. 16 it is included in the reduced values of inductance and resistance), but also connected in parallel with the inductance (as shown in Fig. 10), is of fundamental importance. A special analysis showed that this parallel conductivity cannot be less than the conductivity of a vacuum, determined by its input impedance, and determines the Principle of Certainty of electrical measurements, an analogue of the Heisenberg Uncertainty Principle, but more current. But at finite values of the specific resistances of the medium, we have, as shown in Fig. 12 for a reduced resistance equal to unity, the frequency boundary of the growth of the reflection modulus and phase rotation with increasing inductance.

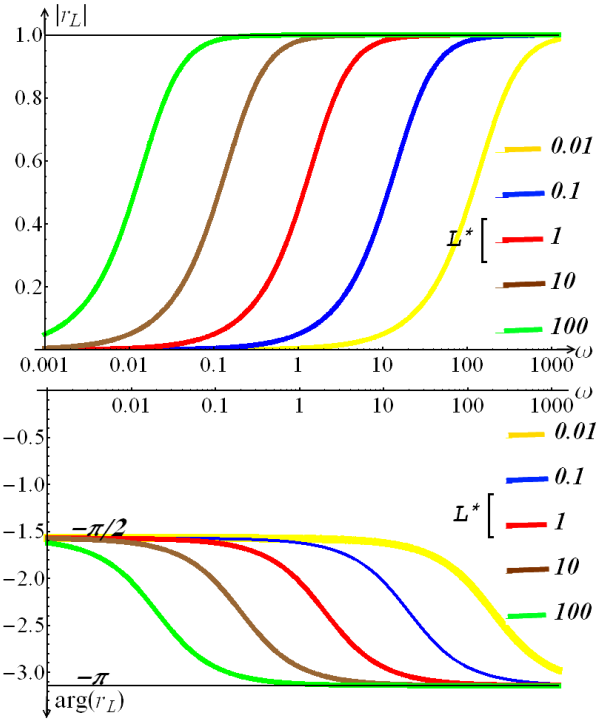

Fig12. *The spectra of the modulus and phase of the reflection coefficient of various inductances at a unit reduced specific resistance*

And so we got that the smaller the reduced inductance, the larger the interval of low frequencies of non-reflection by inductance - $(1-r)$. So the frequency dependence of non-reflection, in principle, correlates with the skin absorption shown in Fig. 8!

We will not carry out a more detailed quantitative analysis of the impedance here. Let us only take into account, also qualitatively, that the spatial scale of the introduced discreteness, determined by the mean free path of electrons, determines the existence of the maximum frequency for electromagnetic waves propagating along the quasi-translated links of the chain. This maximum frequency is determined by the local resonant frequency characteristic of the selected link. So we have, as shown in Fig. 12, a cutoff of the frequency dependence of the reflection coefficient at the plasma frequency - collective plasma oscillations exist on a scale larger than the mean free path of electrons. AndifweusethemodifiedFermi-Diracstatistics:

$$F(\omega)=\frac{1}{Exp\left[\frac{\hbar(\omega-\omega_P)}{kT}\right]+1} \tag{17}$$

then we get a cutoff of the frequency dependences of the reflection coefficient at one (Fig. 13).

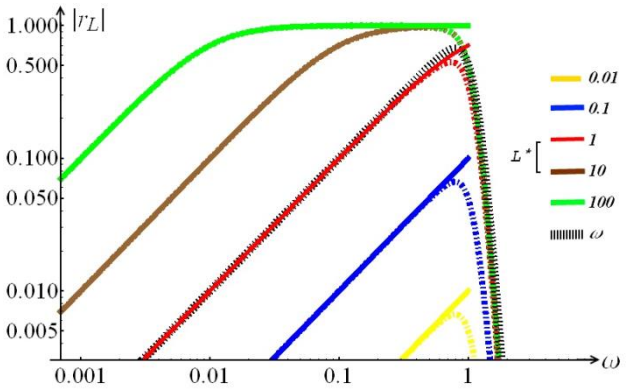

Fig13. *Clipping of the reflection spectra of various inductances at a unit reduced resistivity at the plasma frequency*

Above was given a general scheme of a unified description using the corrected impedance of the reflection of the conducting medium for any frequencies of electromagnetic waves. This scheme, in principle, is also suitable for specific calculations of optical elements for modulation and amplification.

However, there is a simpler technique that qualitatively correctly reflects the contributions of different processes of different sizes, giving factors, which completely retains the dimension of the entire expression and which is in good agreement with the empirical regularities observed in practice - this is the geometric mean shown in Fig. 15 of the dimensionless frequency dependences of absorption of the described above skin (form 12) and plasma (form 11) models.

As seen from Fig. 13, at a low, in comparison with the plasma frequency, the damping frequency of free carriers (at a large mean free path of carriers, which is observed in perfect lightly doped semiconductors), we have an almost pure resonance at zero frequency. Whereas at a large relative damping frequency (small electron mean free path, which we have in metals), we observe a root growth from the absorption frequency, which is characteristic of metals in a wide frequency range.

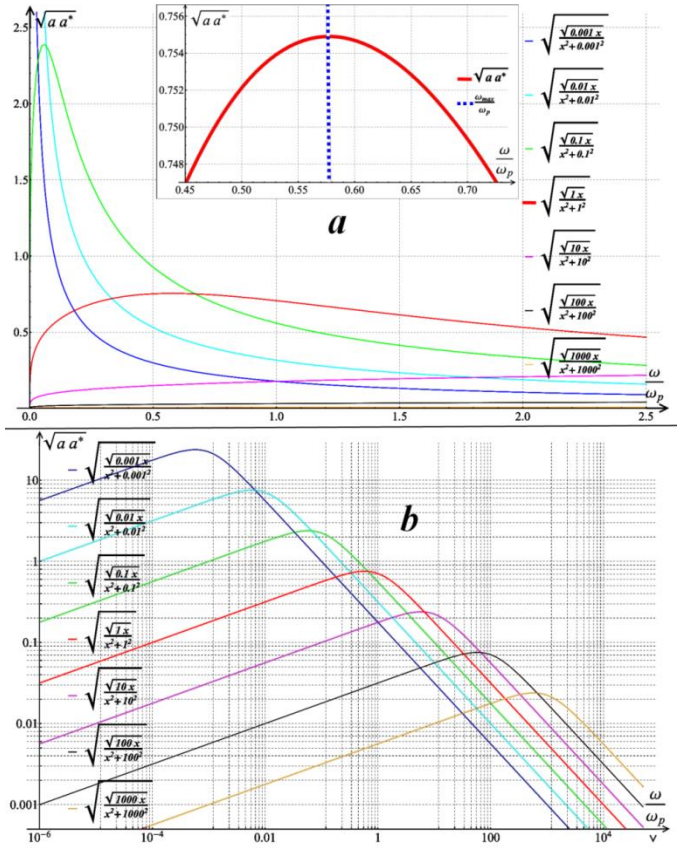

Fig14. *Frequency dependence of the geometric mean skin-plasma absorption*

The geometric mean compilation of absorptions presented in Fig. 13 phenomenologically eliminates the noted catastrophes of the models previously used separately. But it additionally emphasizes that it is necessary to develop a microscopic model that takes into account the spatial characteristics of not only the layer of active (dissipative) attenuation of radiation deep into the reflecting material, but also the spatial characteristics of the layer of reactive attenuation of radiation deep into the interface. In the case of ideal, 100% reflection (following from a purely plasma model at low frequencies), it is the reactive part that is decisive, i.e. the thickness of this layer is greater than the absorption thickness. This microscopic thickness can be estimated in terms of reflection on monoatomic layers using inductance as a model characteristic of electrical conductivity.

4. CONCLUSION

The presented work may seem excessively detailed for theoretical physicists, and insufficiently detailed for experimental physicists who design devices (although I personally divide into physicists and non-physicists). But there is one fundamental BUT!

Planck, eliminating the singularities existing only in "theories", came to the necessity of introducing a new independent (orthogonal) INVARIANT - QUANTUM, and thus to the need to use countable sets. But the development of quantization (not by Planck) followed the path of compilation, and not the path of strict consideration of cross between effects, cross between electric and gravitational [14-18]. So the constructed Quantum Mechanics operates with the Schrödinger equation, which is not INVARIANT, but primitive, roughly describing only hydrogen-like "atoms" [19], which leads to numerous contradictions and to a brake on sciences adjacent to physics [19, 20, 21]. So, in order to justify the details of the presentation in this work, I want to note that in the description of seemingly well-known effects during its implementation, "small" roughnesses were identified, which were neglected as insignificant, but it was precisely their elimination that made it possible to take a step in continuing the work begun by Planck - construction of Quantum Nonmechanics.

REFERENCES

[1] Grosse P., "Free electrons in solids", Springer-Verlag, Berlin-Heidelberg-New York, 1979, 270 pp/

[2] Amnon Yariv, Pochi Yen, “OPTICAL WAVES IN CRISTALS (Propogation and Control of Laser Radiation), A Wiley-InterscіencePablication, John Wiley & Sons? New York/Chichester/Brisbant/ Toronto/Singapure, 1985, 616 pp.

[3] S.V. Ordinets, Plasma reflection of CoSi in the temperature range 80-300 K,Solid State Physics, 1979, v. 20, № 5, p 1541-1544.

[4] M. Born, E. Wolf, PRINCIPLES OF OPTICS, Pergamon Press, Oxford-London-Edinburgh-New York-Paros-Frankfurt, 1964,856 pp.

[5] V.P. Shestopalov, A.A. Kirilenko, S.A. Masalov, Yu.K. Sirenko, Resonant scattering of waves, v.1 - Diffraction gratings, Kiev, "NaukovaDumka", 1986, 232 p.

[6] S.V. Ordin, Giant spatial dispersion in the region of plasmon-phonon interaction in one-dimensional-incommensurate crystal the higher silicide of manganese (HSM)”, in Book: Optical Lattices: Structures, Atoms and Solitons, “, Editors: Benjamin J. Fuentes, Nova Sc. Publ. Inc., 2011, pp. 101-130.

[7] A. A. Vlasov. Chapter VI. Paragraph 5 // Macroscopic electrodynamics. 2nd ed. Moscow, "Science", 2005.

[8] William Hart (2006), Engineering Electromagnetics (7th ed.), New York: McGraw Hill, ISBN 978-0-07-310463-8

[9] Non-destructive testing: reference book: In 7v. Under total. ed. V.V. Klyueva. T. 2: In 2 kn.-M .: Mashinostroenie, 2003.-688 p .: ill.

[10] Arian Rahimi, Yong-Kyu Yoon, Study on Cu/Ni Nano Superlattice Conductors for Reduced RF Loss, IEEE Microwave and Wireless Components Letters, , vol. 26, no. 4, Mar. 16, 2016, pp. 258-260.

[11] Frank S. Grawford, Jr., BERKLEY PHYSICS COURSE, v.III, McGray-Hill Book Company, 1972, 530 pp.

[12] Bessonov LA Theoretical foundations of electrical engineering. - 9th ed. - M .: Higher school, 1996.

[13] Alexander, Charles; Sadik, Matthew (2006). Fundamentals of Electrical Circuits (3, revised ed.). McGraw Hill. S. 387-389. ISBN 978-0-07-330115-0.

[14] Ordin, S.V., Newton's Coulomb Laws, International Journal of Current Advanced Research, Volume 7, Issue 12, December 2018, p. 1-16

[15] Ordin, S.V., «CHAOS – IMAGINARY OSTENSIBILITY – ORTHOGONALITY», Global Journal of Science Frontier Research- Physics & Space Science (GJSFR-A),Volume 19 Issue 3 Version 1.0 p.49-58, https://globaljournals.org/GJSFR_Volume19/3-Chaos-Imaginary-Ostensibility.pdf

[16] Ordin, S.V., «Parametrically excited Anharmonic Oscillator», Global Journal of Science Frontier Research- Physics & Space Science (GJSFR-A),Volume 19 Issue 3 Version 1.0 p.133-144, https://globaljournals.org/GJSFR_Volume19/7-Parametrically-Excited.pdf

[17] Ordin, S.V., «The Schottky Effect and Cosmos»,Global Journal of Science Frontier Research- Physics & Space Science (GJSFR-A), Volume 19 Issue 4 Version 1.0, p.39-50, https://journalofscience.org/ index.php/GJSFR/article/view/2480https://journalofscience.org/index.php/GJSFR/issue/view/399https://globaljournals.org/GJSFR_Volume19/E-Journal_GJSFR_(A)_Vol_19_Issue_4.pdf

[18] Ordin S.V., "The functional relationship of the gravitational and inertial masses." , International Journal of Advanced Research in Physical Science (IJARPS), Volume 6, Issue 6, 2019, PP 24-32,https://www.arcjournals.org/international-journal-of-advanced-research-in-physical-science/volume-6-issue-6/

[19] Ordin S.V., "C & BN-Foundation for Atomic-Crystalline Orbitals", Global Journal of Science Frontier Research- Physics & Space Science (GJSFR-A), Volume 18, Issue 5, Version 1.0, pp. 16-47, https://globaljournals.org/GJSFR_Volume18/E-Journal_GJSFR_(A)_Vol_18_Issue_5.pdf,

[20] Ordin S.V., "Quasinuclear foundation for the expansion of quantum mechanics", International Journal of Advanced Research in Physical Science (IJARPS), Volume 5, Issue 6, 2018, PP 35-45, https://www.arcjournals.org/international-journal-of-advanced-research-in-physical-science/volume-5-issue-6/

[21] Ordin S.V., "Frontier Chemistry Aspects", GJSFR Volume 20 Issue 2 Version 1.0, pp. 1-11, https://globaljournals.org/GJSFR_Volume20/1-Frontier-Chemistry-Aspects.pdf, https://globaljournals.org/latest-ejournals-in-gjsfr